DOI:10.1021/jf900951w

JOURNAL OF AGRICULTURAL AND FOOD CHEMISTRY
ARTICLE

Molecular Binding of Catechins to Biomembranes: Relationship to Biological Activity

Timothy W. Sirk,[†] Eugene F. Brown,[†] Mendel Friedman,[‡] and Amadeu K. Sum*[,§]

[†]Department of Mechanical Engineering, Virginia Polytechnic Institute and State University, Blacksburg, Virginia 24061, [‡]Western Regional Research Center, Agricultural Research Service, U.S. Department of Agriculture, Albany, California 94710, and [§]Department of Chemical Engineering, Colorado School of Mines, Golden, Colorado 80401

Molecular dynamics simulations were used to study the interactions of four green tea catechin compounds with lipid bilayers. Reported studies have shown that catechins are linked to beneficial health effects, specifically those related to interactions with the cell membrane. To better understand the molecular interaction of catechins with membranes, simulations were carried out of interactions of four catechin molecules [epicatechin (EC), epigallocatechin (EGC), epicatechin gallate (ECG), and epigallocatechin gallate (EGCG)] with a 1-palmitoyl-2-oleoylphosphatidylcholine (POPC) lipid bilayer. The simulations show that catechins possess a strong affinity for the lipid bilayer. Some are absorbed into the bilayer. The molecular structure and aggregated condition of the catechins significantly influences their absorption, as well as their ability to form hydrogen bonds with the lipid headgroups. Insight into these molecular interactions helps to distinguish the structure−function relationship of the catechins with lipid bilayers and provides a foundation for a better understanding of the role of catechins in biological processes.

KEYWORDS: Catechin; flavonoid; lipid bilayer; membrane

INTRODUCTION

Flavonoids found in tea have been linked to numerous health benefits. These include antibacterial (*1*, *2*), anticancer (*3*, *4*), anticholesterol (*5*−*7*), antineurodegenerative (*8*), antitoxin (*1*), and antiviral (*9*) effects. For example, our studies have shown that tea catechins and tea extracts inactivated human cancer cells and foodborne pathogens in solution and in ground beef (*3*, *10*, *11*).

Epigallocatechin gallate (EGCG) is the most abundant and powerful antioxidant found in green tea (*12*). However, it should be noted that the levels of this and other catechins may decrease during long-term storage of tea bags (*13*). Large differences in biological activities of structurally different catechins may be due to differences in relative affinities to lipid bilayers of cell membranes. Features of catechins that may influence affinities to cell membranes include stereochemistry, the presence of galloyl side chains, and the number of phenolic OH groups on the catechin rings.

However, the quantitative nature of the molecular interactions of flavonoids or inside cell membranes that may govern biological activities remains largely undefined (*14*−*25*). Recent experimental studies have shown EGCG induced rupture of giant vesicles by binding to their membrane surface (*18*). Because changes to the lipid bilayer membrane can be linked to changes in biological processes, the microscopic and molecular mechanisms associated with this process may be related to the known health benefits of EGCG and other catechins.

*Corresponding author [telephone (303) 273-3873; fax (303) 273-3730; e-mail asum@mines.edu].

Because of incomplete information about the molecular mechanisms involved in both antioxidant and anticarcinogenic activities of tea flavonoids, we were motivated to study the biophysical interactions of these compounds as they interact with lipid bilayers by means of molecular dynamics simulation techniques (*21*). The main objective of the present study was to extend these studies by evaluating the interaction of the following four tea catechins with 1-palmitoyl-2-oleoylphosphatidylcholine (POPC) bilayers: epicatechin (EC), epigallocatechin (EGC), epicatechin gallate (ECG), and epigallocatechin gallate (EGCG). The dynamics of the interactions of the catechins with the lipid bilayers are interpreted in terms of hydrogen bonding and adsorption/absorption phenomena to the lipid bilayer, as influenced by the phenolic hydroxyl and gallate groups associated with the catechin ring structures.

MATERIALS AND METHODS

With the exception of the lipid hydrocarbon tails, which were treated with a united-atom model, an all-atom molecular representation was used for the catechins, lipids, and water. Intermolecular interactions for the lipids and nonbonded interactions (Lennard-Jones and Coulombic potentials) were obtained from a previous study (*26*). The single point charge (SPC) model (*27*) was used for water and the optimized potential for liquid simulations (OPLS) forcefield for all catechin compounds (*28*).

Molecular dynamics simulations were performed using the leapfrog integration scheme with a time step of 2 fs. Short-range van der Waals and electrostatic interactions were cut off at 1.0 nm.

 Published on Web 07/02/2009

The particle mesh Ewald (PME) method was used to correct for long-range electrostatic interactions (*29*, *30*). The LINear Constraint Solver (LINCS) algorithm (*31*) was applied to constrain all bonds in the lipids and catechins, and the SETTLE algorithm (*32*) was used for the water molecules. Periodic boundary conditions were applied in all directions. All simulations were performed in the *NPT* ensemble using the Berendsen weak coupling technique and anisotropic pressure scaling (*33*). The GROMACS 3.3.3 software package (single precision) (*34*−*36*) was used for all simulations running in parallel on Virginia Tech's System X.

All simulations were performed at 310 K and 1 bar, corresponding to a liquid-crystalline state for the POPC bilayer (see REF *37* for details). The stability of the equilibrated bilayer was confirmed from the area per lipid and lipid tail order parameters. These were in agreement with previously reported values for POPC bilayers (*37*). Detailed information regarding the properties of the POPC lipid bilayer can be found elsewhere (*37*).

The systems studied comprised catechins interacting with a model cell membrane as it may occur in a typical cell. The outer leaflet of a mammalian cell membrane typically has a high concentration of phosphatidylcholine (PC) lipid headgroups, illustrated in **Figure 1a**. As an approximation, we considered lipid bilayers composed of POPC. The POPC bilayers contained 144 lipids per leaflet. The lipid bilayers were built by placing the lipids on a grid to form a monolayer and then transposing another monolayer to form a bilayer structure. A total of 11520 water molecules (40 waters/lipid) were added to the lipid bilayer to create a fully hydrated system. The system was initially heated to 450 K for 10 ns, then cooled, and equilibrated at 310 K for 50 ns. The resulting configuration was used for simulations with the catechins.

The equilibrated POPC bilayer was exposed to a solution containing five tea polyphenol molecules for each of the four cases of EC, EGC, ECG, and EGCG (see **Figure 1b** for labeling of the atoms and rings). In each case, the five catechin molecules were positioned and distributed uniformly in the center of the aqueous phase. Unconstrained molecular dynamics simulations were then performed at 310 K and 100 kPa for the systems of catechins, lipids, and water. Each system was simulated for 150 ns.

RESULTS

To characterize the biophysical interactions of the catechins with the lipid bilayer, the simulations for each system were analyzed for dynamic and structural properties. **Figure 2** shows the center-of-mass (COM) molecular trajectories for each of the EC, EGC, ECG, and EGCG molecules. The trajectories illustrate catechins binding to the lipid headgroups near the bilayer surface (adsorption). In many cases, it also depicts penetration into the bilayer interface (absorption). The figure shows that the catechins were initially inserted into the center of the aqueous phase, where they quickly diffused through the aqueous phase to bind with the bilayer surface. All of the catechins interacted with the lipid headgroups on the bilayer surface. Each of the EC and EGC molecules absorbed underneath the bilayer surface during the simulation, whereas only two ECG and two EGCG molecules exhibited similar behavior. The time required for each molecule to penetrate and remain in the bilayer is shown in **Table 1**.

The results indicate that the catechins without the gallate moiety (EC and EGC) penetrated into the bilayer after an average time of 79 and 34 ns, respectively. By contrast, the penetration time for catechins with the gallate moiety (ECG and EGCG) averaged 28 and 43 ns, respectively. **Figure 2** shows that each of the molecules is absorbed into the bilayer from the COM trajectories. Molecules that remained aggregated absorbed more slowly than those unattached to other molecules. Specifically, four EC molecules aggregated into two pairs (see black/red and blue/magenta in **Figure 2a**). All of the aggregated EC molecules absorbed into the bilayer at times >76 ns. This time period is much longer than the 15 ns required for absorption of the nonaggregated EC molecule. Unlike the EC molecules, the larger ECG and EGCG molecules did not absorb into the bilayer while in the aggregated state.

A distinct molecular feature of ECG and EGCG is the presence of the gallate ester moiety. Catechins with the gallate side chain were not absorbed in the aggregated state. Thus, two aggregated ECG molecules (blue/magenta in **Figure 2c**) and two aggregated EGCG molecules (red/black in **Figure 2d**) remained aggregated throughout most of the simulations without being absorbed into the bilayer.

Figure 3 shows the trajectory of the four catechin species as they diffuse along the bilayer surface (the same trajectories as in **Figure 2**, but with displacement projected along the *xy* plane). These trajectories provide insight into the mobility of the catechins. Following adsorption onto the bilayer, the mobilities appear to substantially decrease. Mobilities further decreased after the compounds had been absorbed inside the bilayer. Once absorbed, the catechin molecules are completely enclosed by the lipid headgroups, and their displacements become restricted. For example, **Figure 3d** shows that an EGCG molecule adsorbed onto the bilayer surface (green trajectory) diffuses over an area covering approximately 25 nm^2, whereas an identical absorbed molecule (red trajectory) diffuses around an area of approximately 7 nm^2.

Figure 3 also shows that a similar loss of mobility takes place for many of the catechins after absorption. Each plot shows two circles for each type of catechin: a larger circle encompasses the trajectory of a catechin adsorbed onto the bilayer surface, and a smaller circle encompasses the trajectory in the absorbed state inside the lipid headgroups.

Hydrogen bonds formed between catechins and lipids were monitored to gain a better understanding of interactions along the bilayer surface. A hydrogen bond is defined as the distance between the H-donor and H-acceptor of < 0.35 nm and a donor−hydrogen−acceptor angle of between 120° and 180° (*38*). The present analysis considers catechin hydroxyl groups as H-donors and lipid oxygen groups as H-acceptors (see **Figure 1a** and **1b** for the naming assignment in the PC headgroups and catechins, respectively). Catechins adsorbed on the bilayer surface often formed hydrogen bonds with two of the phosphate oxygen atoms (O9, O10). After absorption, additional interactions occurred with the lipid oxygen atoms deeper inside the bilayer (O16, O33, and O35).

The frequency and distribution of hydrogen bonds formed among the hydroxyl groups in each of the catechins depend on the nature of the interaction with the bilayer. The H-bonds formed by each hydroxyl group were sampled while the catechins were both adsorbed onto and absorbed into the bilayer. **Figure 4** shows that the distribution of H-bonds among the hydroxyl groups is less uniform when the catechins are adsorbed on the bilayer surface compared to those that are absorbed into the bilayer. Even though all hydroxyl groups in the catechins were susceptible to forming hydrogen bonds with the lipids on the bilayer surface, with the exception of EGC, a greater preference for hydrogen bonds occurred with OH1 and OH2. Among the catechins evaluated, EGC exhibited the most abundant adsorbed interaction on the bilayer surface ($> 40\%$ of H-bonds) with the lipids for a single hydroxyl group (OH6). After being absorbed into the bilayer, the H-bonds formed by each catechin are distributed nearly uniformly among the hydroxyl groups. This result shows that after absorption, all hydroxyl groups are nearly equally exposed to form H-bonds. Analysis of the total number of H-bonds formed by each catechin shown in **Table 2** indicates that approximately twice as many H-bonds per hydroxyl group

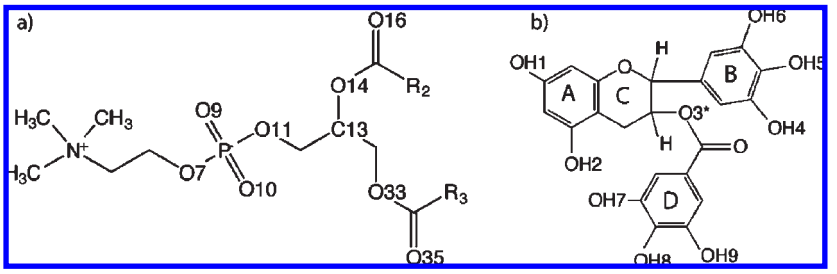

Figure 1. (**a**) Chemical structure of the lipid headgroup and the corresponding oxygen atom numbering assignment. R_2 and R_3 are the oleic acid and palmitic acid tails, respectively. (**b**) Identification of the ring structures and functional groups in the catechins. Phenolic OH donor groups (OH1−OH9) and ring labels (A−D) for catechins are used for reference in the discussions in the text.

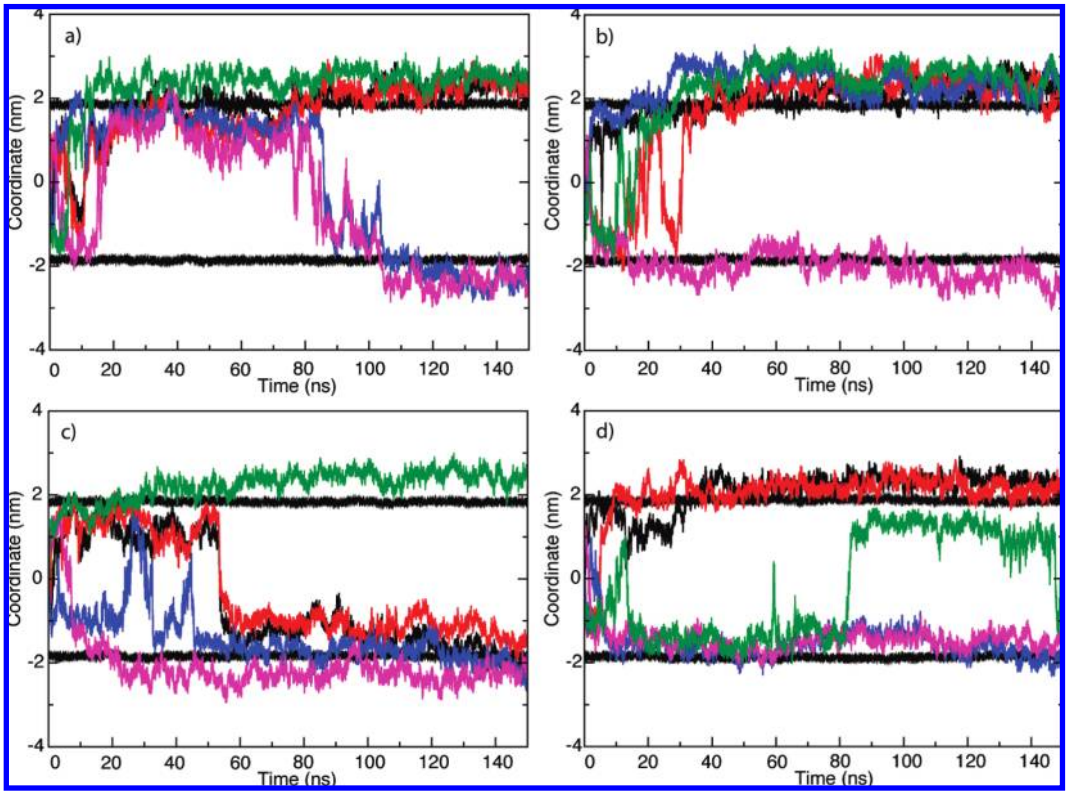

Figure 2. Center of mass trajectories for (**a**) EC, (**b**) EGC, (**c**) ECG, and (**d**) EGCG. The solid black lines represent the average position of the phosphorus atoms in the PC headgroups. Position zero corresponds to the middle of the aqueous phase. Regions above and below the solid black lines correspond to the lipid bilayer. Because of periodic boundary conditions, the catechins can interact with either bilayer surface. Each colored trajectory corresponds to a different catechin molecule.

Table 1. Time Required for Each Catechin in the Simulations To Absorb into the Bilayer[a]

	time (ns) to absorb into the bilayer			
	EC	EGC	ECG	EGCG
black	76	39	N/A[b]	36
red	85	51	N/A	50
blue	116	25	N/A	N/A
magenta	104	26	22	N/A
green	15	28	33	N/A
av	79	34	28[c]	43[c]

[a] Molecule colors correspond to the COM trajectories in **Figure 2**. Here, a molecule is considered to be absorbed into the bilayer when its COM remains below the phosphate group for at least 10 ns. [b] Three ECG and three EGCG molecules did not absorb (N/A). [c] Only absorbed molecules are included in the average.

are formed after the catechins are absorbed into the bilayer, as compared to the number formed following adsorption onto the surface. The ability of all the hydroxyl groups to form H-bonds may be partly responsible for the increase in H-bonds formed after absorption.

The effect of absorption is also apparent when the number of hydroxyl groups that simultaneously form an H-bond is considered. **Figure 5** shows the frequency of the simultaneous H-bonds formed during (**a**) a surface interaction and (**b**) an absorption. For each catechin, the occurrence of multiple H-bonds during a single interaction increased during absorption, that is, more than one hydrogen bond was often formed simultaneously. Except for EGCG, all catechins most likely formed one or two H-bonds on the bilayer surface and four simultaneous H-bonds following absorption. EGCG generally formed five H-bonds. This result is consistent with our previous observation of the unique ability of EGCG, the most active biological catechin, to form H-bonds (*21*). The absorption into the bilayer appears to allow each catechin to increase the number of H-bonds, making all of the hydroxyl groups accessible to the lipid oxygens. Strong hydrogen-bonding

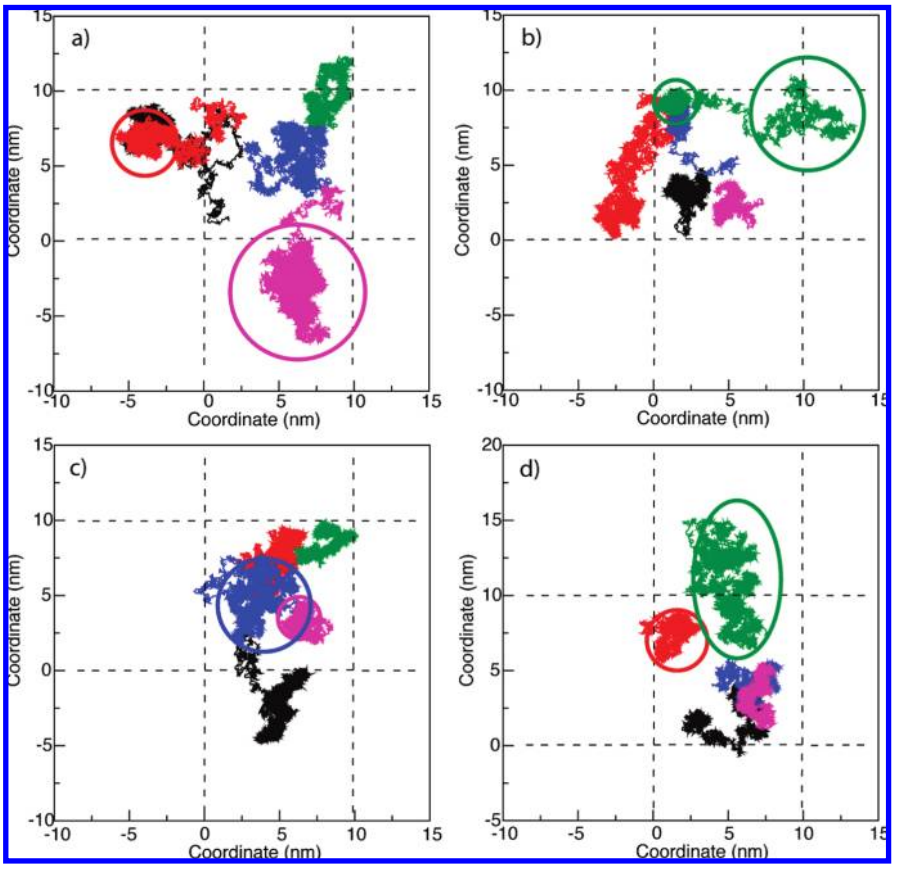

Figure 3. Catechin molecular trajectories along the plane (*xy*) parallel to the bilayer surface. EC, EGC, ECG, and EGCG are shown in **a**, **b**, **c**, and **d**, respectively. Trajectory colors match those shown in **Figure 2**. Dashed line indicates the boundaries of the simulation box. The marked locations (circles) correspond to the time at which the catechin is on the bilayer surface (solid) or adsorbed onto the bilayer (dashed).

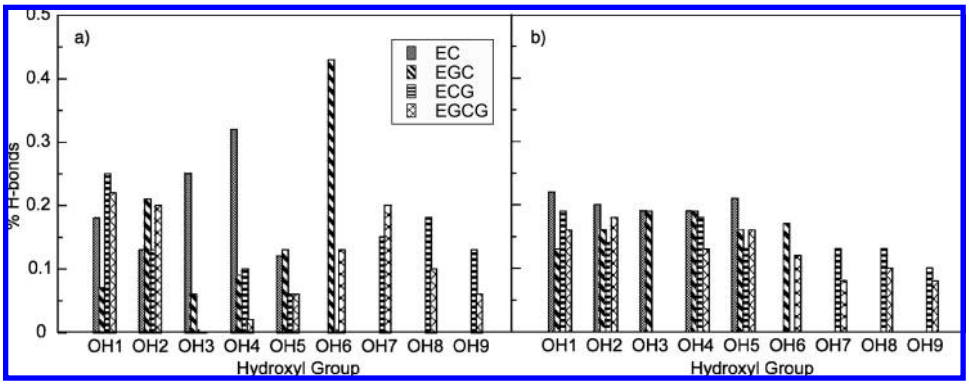

Figure 4. Hydrogen bonds formed by individual hydroxyl donor groups and lipid oxygen acceptors while (**a**) on the surface and (**b**) absorbed into the bilayer. The distribution of H-bonds among the hydroxyl groups is heterogeneous while on the surface, but becomes more uniform following absorption into the bilayer.

interactions presumably initiate the disruption of cell membranes in living cells.

Once absorbed, catechins with a higher number of hydroxyl groups formed a higher number of H-bonds. However, the average number of the H-bonds per hydroxyl group was relatively constant. **Table 2** shows the number of H-bonds formed per hydroxyl group for each catechin as a result of surface interactions and absorption. **Table 2** also shows that catechins on the bilayer surface always formed fewer H-bonds per hydroxyl group than did those that were absorbed into the bilayer, presumably because these catechins had less access to lipid oxygen acceptors inside the bilayer. Because catechins on the surface were often aggregated, some hydroxyl groups were inaccessible to interactions with the bilayer.

Table 2. Ability of Catechins To Form H-Bonds with the Lipid Headgroups Near the Bilayer Surface and Inside the Bilayer Is Quantified by Counting the Number of H-Bonds Formed per Hydroxyl Group per Nanosecond[a]

	EC	EGC	ECG	EGCG
adsorbed	117	152	132	159
absorbed	319	299	260	290

[a] Most catechins formed approximately twice as many H-bonds while absorbed into the lipid headgroups compared to being adsorbed on the surface. The presence of OH6 hydroxyl group increases the ability of catechins to hydrogen bond on the bilayer surface. After being absorbed, the smallest catechins (EC and EGC) formed more H-bonds per hydroxyl group than the catechins with the gallate moiety.

These results indicate that the presence of the gallate moiety (ring D) in ECG and EGCG had a significant impact on how the

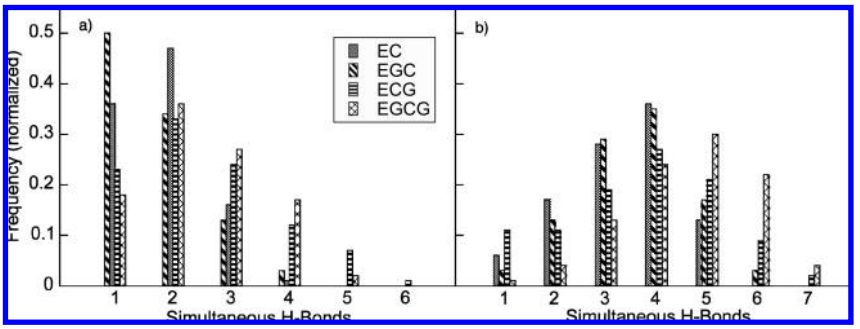

Figure 5. Number of hydrogen bonds formed simultaneously by hydroxyl groups in the catechins (donors) and lipid oxygen atoms (acceptors) while (**a**) on the surface and (**b**) absorbed into the bilayer. While on the surface, catechins typically formed one (EC) or two (EGC, ECG, EGCG) hydrogen bonds. Following absorption, the catechins most often formed four (EC, EGC, ECG) or five (EGCG) hydrogen bonds.

catechins interact with the bilayer. The gallate moiety provides more hydroxyl groups (seven for ECG, eight for EGCG) to form H-bonds. However, the presence of ring D also prevented three of the five ECG and EGCG molecules from being absorbed into the bilayer. Thus, catechins with the OH6 group present formed 30% (EGC) and 20% (EGCG) more H-bonds during surface interactions than did those without the OH6 group.

Catechin hydroxyl donors preferred to form hydrogen bonds with particular lipid acceptors. To determine the most frequently interacting donor−acceptor pairs, the number of H-bonds for each donor−acceptor pair was counted over the course of the simulation. A qualitative summary of these data is provided as Supporting Information. These data suggest that catechin hydroxyl donor groups often have a strong preference for lipid acceptors O9, O10, and O16. They have no significant preference for specific catechin hydroxyl groups.

The absorption of catechins into the bilayer resulted in a lateral expansion of the bilayer. To quantify this expansion, the cross-sectional area occupied by each lipid and by the catechins was estimated at five time periods during the simulation (50, 75, 100, 125, and 150 ns). The EC molecule occupied an area (1.47 nm^2) slightly larger than two lipids, whereas the EGC, ECG, and EGCG molecules occupied an average area of 1.72, 1.98, and 1.80 nm^2, respectively. Although the molecules with the gallate moiety (ECG and EGCG) occupied a larger area per molecule, the largest total area resulted from the absorption of EGC, which does not have the gallate moiety. All five EGC molecules were absorbed into one bilayer leaflet (see **Figure 2b**) and compressed the average area per lipid of the leaflet to about 0.61 nm^2. The area occupied by lipids adjacent to the absorbed catechins experienced the greatest contraction.

Table 3 compares the area occupied by lipids adjacent to the absorbed catechins relative to the areas of all other lipids in the bilayer. Lipids adjacent to the absorbed catechins occupied on average an area one-fourth smaller than other lipids in the bilayer. An example of the area occupied by the catechins and the contraction of nearby lipids is illustrated in **Figure 6**. This figure shows three snapshots of EGCG molecules (black), adjacent lipids (red), and other lipids (white) on a bilayer leaflet at 50, 100, and 150 ns. The low mobility of the catechins after absorption (see above) can be seen by the nearly stationary position of the EGCG molecules.

The ability of catechins on the bilayer surface to interact with multiple lipids was examined by considering the configuration of hydroxyl groups. A Vonoroi tessellation analysis of the lipids was created at 25, 50, 75, 100, 125, and 150 ns for each catechin species. The catechin hydroxyl oxygens were projected onto the tessellations to establish the number of lipids accessible to one catechin molecule. **Figure 7** shows the positions of the hydroxyl groups for two EGCG molecules on the bilayer surface at 25 ns. In this frame, the two molecules overlapped with a total of 10 lipids (an average of 5 lipids per EGCG molecule). When the data from all six time instances for each catechin are considered, the number of lipids associated with the catechins increased as the number of hydroxyl groups increased as follows: (a) EC, the catechin with the least number of hydroxyl groups, overlapped with an average of 3.0 lipids; (b) EGCG, the catechin with the greatest number of hydroxyl groups, overlapped with an average of 4.0 lipids; and (c) EGC and ECG overlapped with averages of 3.3 and 3.7 lipids, respectively. These results suggest that catechins with a high number of hydroxyl groups (such as EGCG) have the potential to interact with a high number of lipid molecules.

Table 3. Average Area per Lipid (in nm^2) for Lipids Adjacent to the Absorbed Catechins and for All Others in the Leaflet[a]

	EC			EGC			ECG			EGCG		
time (ns)	AL	OL	box	AL	OL	box	AL	OL	box	AL	OL	box
50	0.48	0.65	0.65	0.52	0.64	0.67	0.51	0.65	0.65	0.51	0.65	0.66
75	0.49	0.66	0.66	0.49	0.64	0.66	0.52	0.66	0.67	0.49	0.65	0.65
100	0.47	0.66	0.66	0.47	0.64	0.65	0.48	0.65	0.66	0.49	0.65	0.65
125	0.49	0.66	0.66	0.52	0.63	0.66	0.50	0.65	0.66	0.50	0.66	0.65
150	0.54	0.66	0.67	0.48	0.64	0.65	0.47	0.66	0.66	0.56	0.64	0.66
av	0.49	0.66	0.66	0.50	0.64	0.66	0.49	0.66	0.66	0.51	0.65	0.65

[a] Areas are calculated from Vonoroi tessellation analysis at 50, 75, 100, 125, and 150 ns. The area per lipid for adjacent lipids (AL) was about 22−25% smaller than the areas for the other lipids (OL). The overall area per lipid, computed from the area of the bilayer divided by the number of lipids (144), is shown as "box".

The presence of the gallate moiety allows ECG and EGCG to access an average of 0.7 additional lipid as compared to EC and EGC, which do not have gallate side chains. OH4 allows EGC and EGCG to access an average of 0.3 additional lipid relative to EC and ECG.

DISCUSSION

Impact of Catechins on Lipid Bilayers. The described simulations demonstrate the impact of catechin interactions with a POPC bilayer. All of the catechins interacted strongly with the bilayer. However, catechins without the gallate moiety (EC and EGC) absorbed into the bilayer to a greater extent than did those with the gallate moiety (ECG and EGCG). This difference may be due to, in part, to the inability of aggregated ECG and EGCG molecules to absorb into the bilayer. After absorption into the bilayer occurred, all catechins caused a lateral expansion in the bilayer below the phosphate group of the lipid chain.

It has been suggested that the beneficial health effects of EGCG and other catechins are due in part to induced changes

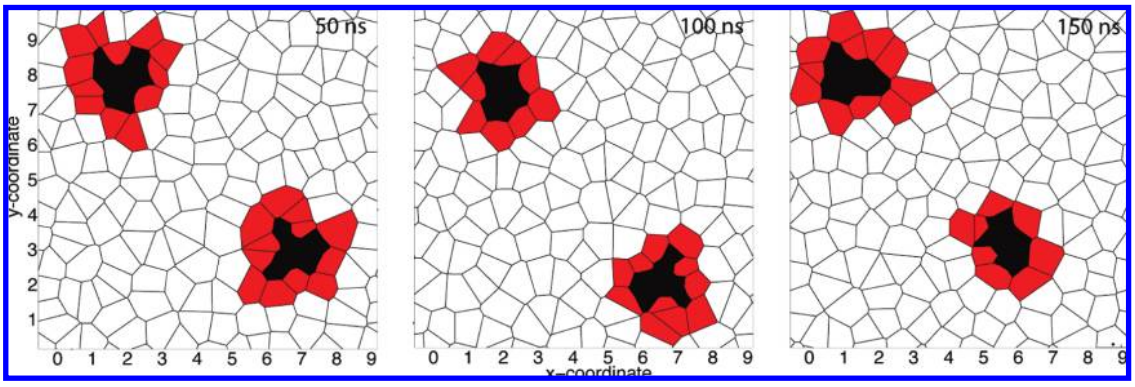

Figure 6. Cross-sectional areas occupied by EGCG on a plane near the C13 carbon (see **Figure 1a**). Each plot represents a snapshot in time of one bilayer leaflet at 50, 100, and 150 ns. The area of the catechins (black), lipids adjacent to the catechins (red), and other lipids (white) are estimated from the Voronoi tessellation analysis.

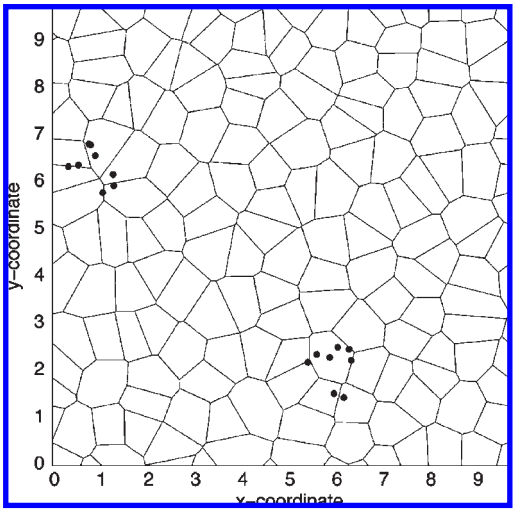

Figure 7. Interaction of two EGCG molecules on the bilayer surface after 25 ns. Hydroxyl oxygen atoms (represented as dark circles) are projected onto the Vonoroi tessellation plot representing the lipids. The number of lipids overlapped by the hydroxyl oxygen atoms indicates how many interactions (such as H-bonds) are possible with different lipids. The two EGCG molecules shown overlap with four and six lipids.

in the bilayer structure (*15*, *16*, *18*, *19*, *23*, *39*–*42*). In addition, a recent study reported that EGCG ruptured giant vesicles (*18*). This was also likely caused by the absorption of EGCG and the expansion of the lipid bilayer. A related study showed that a lipid bilayer experienced an expansion of 0.374 nm^2 for each bound EGCG molecule (*41*).

We observed EGCG to occupy a lateral area significantly greater than 0.374 nm^2 (see **Table 3**). However, our simulations show that the lateral expansion of the bilayer is a result of both the lateral area taken up by EGCG molecules and the contraction of the lipids adjacent to the EGCG molecule. We found that an average of 10.8 lipids is adjacent to each absorbed EGCG molecule. Thus, **Table 3** shows that each lipid adjacent to EGCG occupies an area of about 0.51 nm^2 (0.14 nm^2 less area than other lipids). These adjacent lipids therefore introduce an area contraction of $10.8 \times 0.14 = 1.5$ nm^2. The bilayer expansion resulting from a single EGCG molecule can be computed by subtracting the contraction of the adjacent lipids (1.5 nm^2) from the area of one EGCG molecule (1.8 nm^2). The result of 0.3 nm^2 is similar to that observed by Sun et al. (*41*).

Aggregation of Catechins in the Lipid Bilayer. In the present study, we observed aggregation for EC, ECG, and EGCG molecules. Compared with nonaggregated molecules, these aggregated molecules remained adsorbed on the bilayer surface for an increased time period. These observations suggest that the aggregated molecules either absorbed more slowly into the lipid headgroups (EC) or were not absorbed (ECG, EGCG).

The aggregation of catechins, especially EGCG, has also been observed by other investigators (*43*). For example, partition coefficients of EGCG have been reported to decrease with increasing concentration (*41*), a behavior that could be related to the aggregation of solute molecules. Experiments involving the interaction of catechins with the gallate moiety (such as EGCG or ECG) have shown that, when EC is present, more EGCG is incorporated into the bilayer. However, the presence of other catechins does not affect the absorption of EC (*43*). These authors suggested that EC reduces the aggregation of ECG and EGCG, thus allowing a more intimate interaction with the bilayer. We also observed that aggregated ECG and EGCG molecules were not easily absorbed into the bilayer compared with the nonaggregated counterparts.

An alternative explanation for the experimental findings is that after being incorporated into the bilayer, EC then forces local density changes of the lipid headgroups (as shown in **Table 1**). The sequence of events facilitates EGCG's entry into the bilayer. Several studies that have shown that EGCG accumulations on the bilayer surface are consistent with our results, which showed that three of the five EGCG molecules remained on the bilayer surface. For example, a previous study has suggested that the partitioning of EGCG into lipid bilayers increases as the density of PC lipids decrease (*44*). The present study shows that smaller catechin molecules (EC, EGC) absorb into the bilayer more readily than larger catechins (ECG, EGCG). This finding suggests that an increase of catechin size relative to gaps in the lipids in the bilayer can delay or prevent the absorption of some catechins.

Effects of Catechins on Hydrogen Bonding on the Surface and within the Lipid Bilayer. Hydrogen bonding of hydroxyl groups with lipid acceptors is an important factor in catechin interactions with the bilayer. While on the bilayer surface catechins formed H-bonds with only a few of the available hydroxyl groups. Following absorption, the distribution of H-bonds among hydroxyl groups became much more uniform; more H-bonds were formed simultaneously and at an increased rate. This series of events is likely due to differences in accessibilities of different hydroxyl groups to lipid acceptors. In addition, the rate of H-bonding also increased with an increasing number of hydroxyl groups. These results support the previously reported linear relationship between the number of catechin hydroxyl groups and bilayer retention times (*45*).

Relationship of Hydrogen Bonding to Biological Activities of Catechins. A theoretical study by Tejero et al. (*46*) using variational transitional state theory suggests that the antioxidant activity of catechins is associated with the formation of hydrogen bonds between two OH groups of the catechol moiety and two oxygen atoms of lipid peroxy radicals, resulting in the formation of a very compact reactant complex. This observation and the present study suggest that hydrogen-bonding effects may govern both antioxidative and cell membrane disruptive effects of catechins.

A key question is whether biological effects of catechins parallel hydrogen bonding effects with cell membranes. The following observations suggest that this appears to be the case. Previously, we found that relative antimicrobial activities of six catechins against the foodborne pathogen *Bacillus cereus* ranged as follows: gallocatechin, 1.0; epigallocatechin, 1.2; epicatechin-3-gallate, 45; catechin-3-gallate, 180; epigallocatechin-3-gallate, 1459; and gallocatechin-3-gallate, 2307 (*10*). A related study showed that the activities of the same catechins paralleled inhibitory effects against human cancer cells (*3*). These observations indicate that the gallate ester side chains enhance biological effects of catechins and that hydrogen bonding of the catechins with lipid bilayers of cell membranes described in our previous (*21*) and present studies seem to generally parallel antimicrobial and anticancer effects.

However, because in vivo bioavailability of catechins (fraction of catechins that reaches the circulation) is low and is influenced by other dietary ingredients such as piperine (*47*) and the additional fact that nongallated catechins appear to be more bioavailable than are 3-gallated ones (*48*−*50*), in vitro results may not always predict in vivo effects.

The situation is even more complicated by contributions of biotransformed metabolites (due to the action of colonic microflora and metabolizing enzymes) to biological activities (*51*). It is also relevant to note that consumers who dislike the astringent somewhat bitter taste of many teas have the option of obtaining sweet-tasting high-catechin pan-fried tea largely unavailable in Western countries (*52*).

Conclusions. This study presents results from molecular dynamics simulations on the interactions of four tea catechins with a lipid bilayer. All four catechins were attracted to the lipid bilayer surface and were mobile along the surface. However, after being absorbed, they were essentially trapped between the lipid molecules, and their movement within the bilayer was restricted. In the absorbed state, the catechins both expanded the bilayer by displacing lipid headgroups and caused a contraction in the headgroup area of adjacent lipids. Although the behavior of the lipid tails was not investigated here, the smaller headgroup areas of those lipids adjacent to absorbed catechins could result in reduced thermal motion of the lipid tails and a corresponding more ordered local lipid environment. The lateral expansion of the bilayer resulting from the absorption of a single EGCG molecule was similar to that observed by other investigators (*41*). The time required for the catechins to be incorporated into the lipid bilayer was related to the structural properties and aggregated condition of the molecules. Aggregated catechins either absorbed more slowly (EC) than their nonaggregated counterparts or were not absorbed at all (ECG, EGCG). The two aggregated catechins that were not absorbed contained gallate side chains and had the largest molecular weights.

The frequency of hydrogen bond formation between the catechins and the lipid bilayer increased for catechins that were absorbed into the bilayer as compared to those that interacted only with the bilayer surface. In the absorbed state, the catechin hydroxyl groups were better able to access lipid oxygen acceptors and form additional hydrogen bonds with the bilayer. Our results support observations by other investigators that the number of hydrogen bonds increases with the number of hydroxyl groups.

EGCG occurs at high concentrations in green teas and is one of the most biologically active and studied catechins. Our results show that EGCG readily forms hydrogen bonds with lipid bilayers. This catechin formed the most hydrogen bonds while on the bilayer surface as well after being absorbed into the bilayer. In addition, our simulations also indicate that the presence of the gallate moiety in EGCG and ECG facilitates the formation of multiple hydrogen bonds and support recent studies showing that catechins with the gallate moiety have a much larger affinity for lipid bilayers than those without, such as EC or EGC (*39*, *53*).

These observations suggest the need to also subject biologically active black tea theaflavins (theaflavin, theaflavin-3-gallate, theaflavin-3′-gallate, and the theaflavin-3,3′-digallate), oxidation dimers of catechins with a large number of OH groups and gallate side chains, to analogous molecular modeling and simulations with lipid bilayers of cell membranes.

In conclusion, the results presented here complement and extend the current knowledge of catechin-cell membrane interactions. The described findings are of fundamental interest and may facilitate understanding of the structure−function relationship of the catechins to their bioactivity as governed by the lipid bilayer interactions and as they affect numerous biochemical, pharmacological, and medicinal properties of green tea catechins and possibly other polyphenolic compounds.

ACKNOWLEDGMENT

Computational resources were provided by the Virginia Tech Advanced Research Computing Facility (System X).

Supporting Information Available: Chemical structure for catechins, and hydrogen bonding between catechins (donor) and lipids (acceptor). This material is available free of charge via the Internet at http://pubs.acs.org.

LITERATURE CITED

(1) Friedman, M. Overview of antibacterial, antitoxin, antiviral, and antifungal activities of tea flavonoids and teas. *Mol. Nutr. Food Res.* **2007**, *51*, 116–134.

(2) Sharangi, A. B. Medicinal and therapeutic potentialities of tea (*Camellia sinensis* L.)—a review. *Food Res. Int.* **2009**, in press.

(3) Friedman, M.; Mackey, B. E.; Kim, H. J.; Lee, I. S.; Lee, K. R.; Lee, S. U.; Kozukue, E.; Kozukue, N. Structure−activity relationships of tea compounds against human cancer cells. *J. Agric. Food Chem.* **2007**, *55*, 243–253.

(4) Shimizu, M.; Fukutomi, Y.; Ninomiya, M.; Nagura, K.; Kato, T.; Araki, H.; Suganuma, M.; Fujiki, H.; Moriwaki, H. Green tea extracts for the prevention of metachronous colorectal adenomas: a pilot study. *Cancer Epidemiol. Biomarkers Prev.* **2008**, *17*, 3020–3025.

(5) He, R.-R.; Chen, L.; Lin, B.-H.; Matsui, Y.; Yao, X.-S.; Kurihara, H. Beneficial effects of oolong tea consumption on diet-induced overweight and obese subjects. *Chin. J. Integr. Med.* **2009**, *15*, 34–41.

(6) Pearson, D. A.; Frankel, E. N.; Aeschbach, R.; German, J. B. Inhibition of endothelial cell mediated low-density lipoprotein oxxidation by green tea extracts. *J. Agric. Food Chem.* **1998**, *46*, 1445–1449.

(7) Frankel, E. N.; Huang, S.-W.; Aeschbach, R. Antioxidant activity of green teas in different lipid systems. *J. Am. Oil Chem. Soc.* **1997**, *74*, 1309–1315.

(8) Mandel, S. A.; Amit, T.; Weinreb, O.; Reznichenko, L.; Youdim, M. B. H. Simultaneous manipulation of multiple brain targets by green tea catechins: a potential neuroprotective strategy for Alzheimer and Parkinson diseases. *CNS Neurosci. Ther.* **2008**, *14*, 352–365.

(9) Isaacs, C. E.; Wen, G. Y.; Xu, W.; Jun, H. J.; Rohan, L.; Corbo, C.; Di Maggio, V.; Jenkins, E. C. Jr.; Hillier, S. Epigallocatechin gallate inactivates clinical isolates of herpes simplex virus. *Antimicrob. Agents Chemother*. **2008**, *52*, 962–970.
(10) Friedman, M.; Henika, P. R.; Levin, C. E.; Mandrell, R. E.; Kozukue, N. Antimicrobial activities of tea catechins and theaflavins and tea extracts against *Bacillus cereus*. *J. Food Prot*. **2006**, *69*, 354–361.
(11) Juneja, V. K.; Bari, M. L.; Inatsu, Y.; Kawamoto, S.; Friedman, M. Thermal destruction of *Escherichia coli* O157:H7 in *sous-vide*-cooked ground beef as affected by tea leaf and apple skin powders. *J. Food Prot*. **2009**, *72*, 860–865.
(12) Friedman, M.; Kim, S.-Y.; Lee, S.-J.; Han, G.-P.; Han, J.-S.; Lee, R.-K.; Kozukue, N. Distribution of catechins, theaflavins, caffeine, and theobromine in 77 teas consumed in the United States. *J. Food Sci*. **2005**, *70*, C550–559.
(13) Friedman, M.; Levin, C. E.; Lee, S.-U.; Kozukue, N. Stability of green tea catechins in commercial tea leaves during storage for 6 months. *J. Food Sci*. **2009**, *74*, H47–H51.
(14) Chen, L.; Yang, X.; Jiao, H.; Zhao, B. Tea catechins protect against lead-induced cytotoxicity, lipid peroxidation, and membrane fluidity in HepG2 cells. *Toxicol. Sci*. **2002**, *69*, 149–156.
(15) Kajiya, K.; Kumazawa, S.; Nakayama, T. Steric effects on interaction of tea catechins with lipid bilayers. *Biosci., Biotechnol., Biochem*. **2001**, *65*, 2638–2643.
(16) Kumazawa, S.; Kajiya, K.; Naito, A.; Saito, H.; Tuzi, S.; Tanio, M.; Suzuki, M.; Nanjo, F.; Suzuki, E.; Nakayama, T. Direct evidence of interaction of a green tea polyphenol, epigallocatechin gallate, with lipid bilayers by solid-state nuclear magnetic resonance. *Biosci., Biotechnol., Biochem*. **2004**, *68*, 1743–1747.
(17) Nakayama, T.; Ono, K.; Hashimoto, K. Affinity of antioxidative polyphenols for lipid bilayers evaluated with a liposome system. *Biosci., Biotechnol., Biochem*. **1998**, *62*, 1005–1007.
(18) Tamba, Y.; Ohba, S.; Kubota, M.; Yoshioka, H.; Yoshioka, H.; Yamazaki, M. Single GUV method reveals interaction of tea catechin (2)-epigallocatechin gallate with lipid membranes. *Biophys. J*. **2007**, *92*, 3178–3194.
(19) Yoshioka, H.; Haga, H.; Kubota, M.; Sakai, Y. Interaction of (+)-catechin with a lipid bilayer studied by the spin probe method. *Biosci., Biotechnol., Biochem*. **2006**, *70*, 395–400.
(20) Tsuchiya, H.; Tanaka, T.; Nagayama, M. Antiproliferative effects associated with membrane lipid interaction of green tea catechins. *J. Health Sci*. **2008**, *54*, 576–580.
(21) Sirk, T. W.; Brown, E. F.; Sum, A. K.; Friedman, M. Molecular dynamics study on the biophysical interactions of seven green tea catechins with lipid bilayers of cell membranes. *J. Agric. Food Chem*. **2008**, *56*, 7750–7758.
(22) Kajiya, K.; Kumazawa, S.; Naito, A.; Nakayama, T. Solid-state NMR analysis of the orientation and dynamics of epigallocatechin gallate, a green tea polyphenol, incorporated into lipid bilayers. *Magn. Reson. Chem*. **2008**, *46*, 174–177.
(23) Uekusa, Y.; Kamihira, M.; Nakayama, T. Dynamic behavior of tea catechins interacting with lipid membranes as determined by NMR spectroscopy. *J. Agric. Food Chem*. **2007**, *55*, 9986–9992.
(24) Kubota, M.; Haga, H.; Takeuchi, Y.; Okuno, K.; Yoshioka, H.; Yoshioka, H. Effect of tea catechins on the structure of lipid membrane and beta-ray induced lipid peroxidation. *J. Radioanal. Nucl. Chem*. **2007**, *272*, 571–574.
(25) Fujihara, T.; Nakagawa-Izumi, A.; Ozawa, T.; Numata, O. High-molecular-weight polyphenols from oolong tea and black tea: purification, some properties, and role in increasing mitochondrial membrane potential. *Biosci., Biotechnol., Biochem*. **2007**, *71*, 711–719.
(26) Leekumjorn, S.; Wu, Y.; Sum, A. K.; Chan, C. Experimental and computational studies investigating trehalose protection of HepG2 cells from palmitate-induced toxicity. *Biophys. J*. **2008**, *94*, 2869–2883.
(27) Berendsen, H. J. C.; Postma, J. P. M.; Van Gunsteren, W. F.; Hermans, J. Interaction models for water in relation to protein hydration. In *Intermolecular Forces*; Pullman, B., Ed.; Reidel Publishing: Dordrecht, The Netherlands, 1981; pp 331−342.
(28) Jorgensen, W. L.; Maxwell, D. S.; Tirado-Rives, J. Development and testing of the OPLS all-atom force field on conformational energetics and properties of organic liquids. *J. Am. Chem. Soc*. **1996**, *118*, 11225–11236.
(29) Darden, T.; York, D.; Pedersen, L. Particle mesh Ewald: an N·log (N) method for Ewald sums in large systems. *J. Chem. Phys*. **1993**, *98*, 10089–10092.
(30) Essmann, U.; Perera, L.; Berkowitz, M. L.; Darden, T.; Lee, H.; Pedersen, L. G. A smooth particle mesh Ewald method. *J. Chem. Phys*. **1995**, *103*, 8577–8593.
(31) Mazur, A. K. Quasi-Hamiltonian equations of motion for internal coordinate molecular dynamics of polymers. *J. Comput. Chem*. **1997**, *18*, 1354–1364.
(32) Miyamoto, S.; Kollman, P. A. SETTLE: an analytical version of the SHAKE and RATTLE algorithms for rigid water models. *J. Comput. Chem*. **1992**, *13*, 952–962.
(33) Berendsen, H. J. C.; Postma, J. P. M.; Van Gunsteren, W. F.; Dinola, A.; Haak, J. R. Molecular dynamics with coupling to an external bath. *J. Chem. Phys*. **1984**, *81*, 3684–3690.
(34) Lindahl, E.; Hess, B.; van der Spoel, D. GROMACS 3.0: A package for molecular simulation and trajectory analysis. *J. Mol. Model*. **2001**, *7*, 306–317.
(35) Berendsen, H. J. C.; van der Spoel, D.; van Drunen, R. GROMACS: a message-passing parallel molecular dynamics implementation. *Comput. Phys. Commun*. **1995**, *91*, 43–56.
(36) Van Der Spoel, D.; Lindahl, E.; Hess, B.; Groenhof, G.; Mark, A. E.; Berendsen, H. J. C. GROMACS: Fast, flexible, and free. *J. Comput. Chem*. **2005**, *26*, 1701–1718.
(37) Leekumjorn, S.; Sum, A. K. Molecular characterization of gel and liquid-crystalline structures of fully hydrated POPC and POPE bilayers. *J. Phys. Chem. B* **2007**, *111*, 6026–6033.
(38) Brady, J. W.; Schmidt, R. K. The role of hydrogen bonding in carbohydrates: molecular dynamics simulations of maltose in aqueous solution. *J. Phys. Chem*. **1993**, *97*, 958–966.
(39) Caturla, N.; Vera-Samper, E.; Villalain, J.; Mateo, C. R.; Micol, V. The relationship between the antioxidant and the antibacterial properties of galloylated catechins and the structure of phospholipid model membranes. *Free Radical Biol. Med*. **2003**, *34*, 648–662.
(40) Nagle, D. G.; Ferreira, D.; Zhou, Y. D. Epigallocatechin-3-gallate (EGCG): chemical and biomedical perspectives. *Phytochemistry* **2006**, *67*, 1849–1855.
(41) Sun, Y.; Hung, W. C.; Chen, F. Y.; Lee, C. C.; Huang, H. W. Interaction of tea catechin (−)-epigallocatechin gallate with lipid bilayers. *Biophys. J*. **2009**, *96*, 1026–1035.
(42) Tsuchiya, H. Effects of green tea catechins on membrane fluidity. *Pharmacology* **1999**, *59*, 34–44.
(43) Kajiya, K.; Kumazawa, S.; Nakayama, T. Effects of external factors on the interaction of tea catechins with lipid bilayers. *Biosci., Biotechnol., Biochem*. **2002**, *66*, 2330–2335.
(44) Kitano, K.; Nam, K. Y.; Kimura, S.; Fujiki, H.; Imanishi, Y. Sealing effects of (−)-epigallocatechin gallate on protein kinase C and protein phosphatase 2A. *Biophys. Chem*. **1997**, *65*, 157–164.
(45) Ollila, F.; Halling, K.; Vuorela, P.; Vuorela, H.; Slotte, J. P. Characterization of flavonoid−biomembrane interactions. *Arch. Biochem. Biophys*. **2002**, *399*, 103–108.
(46) Tejero, I.; González-García, N.; González-Lafont, A.; Lluch, J. M. Tunneling in green tea: Understanding the antioxidant activity of catechol-containing compounds. A variational transition-state theory study. *J. Am. Chem. Soc*. **2007**, *129*, 5846–5854.
(47) Lambert, J. D.; Hong, J.; Kim, D. H.; Mishin, V. M.; Yang, C. S. Piperine enhances the bioavailability of the tea polyphenol (−)-epigallocatechin-3-gallate in mice. *J. Nutr*. **2004**, *134*, 1948–1952.
(48) Hackman, R. M.; Polagruto, J. A.; Zhu, Q. Y.; Sun, B.; Fujii, H.; Keen, C. L. Flavanols: digestion, absorption and bioactivity. *Phytochem. Rev*. **2008**, *7*, 195–208.
(49) Henning, S. M.; Choo, J. J.; Heber, D. Nongallated compared with gallated flavan-3-ols in green and black tea are more bioavailable. *J. Nutr*. **2008**, *138*, 1529S–1534S.
(50) Yang, C. S.; Sang, S.; Lambert, J. D.; Lee, M.-J. Bioavailability issues in studying the health effects of plant polyphenolic compounds. *Mol. Nutr. Food Res*. **2008**, *52*, S139–S151.

(51) Lambert, J. D.; Sang, S.; Yang, C. S. Biotransformation of green tea polyphenols and the biological activities of those metabolites. *Mol. Pharm*. **2007**, *4*, 819–825.
(52) Friedman, M.; Levin, C. E.; Choi, S.-H.; Lee, S.-U.; Kozukue, N. Changes in the composition of raw tea leaves from the Korean Yabukida plant during high-temperature processing to pan-fried Kamairi-cha green tea. *J. Food Sci.* **2009**, *74*, C406−C412.
(53) Kamihira, M.; Nakazawa, H.; Kira, A.; Mizutani, Y.; Nakamura, M.; Nakayama, T. Interaction of tea catechins with lipid bilayers investigated by a quartz-crystal microbalance analysis. *Biosci. Biotechnol. Biochem*. **2008**, *72*, 1372–1375.

Received March 20, 2009. Revised manuscript received May 21, 2009. Accepted June 17, 2009. T.W.S. acknowledges financial support provided by the Virginia Tech College of Engineering Dean's Graduate Teaching Fellowship. A.K.S. gratefully acknowledges support from DuPont through a DuPont Young Professor Award.